Supplemental Information:

Supplemental Figures and Legends:

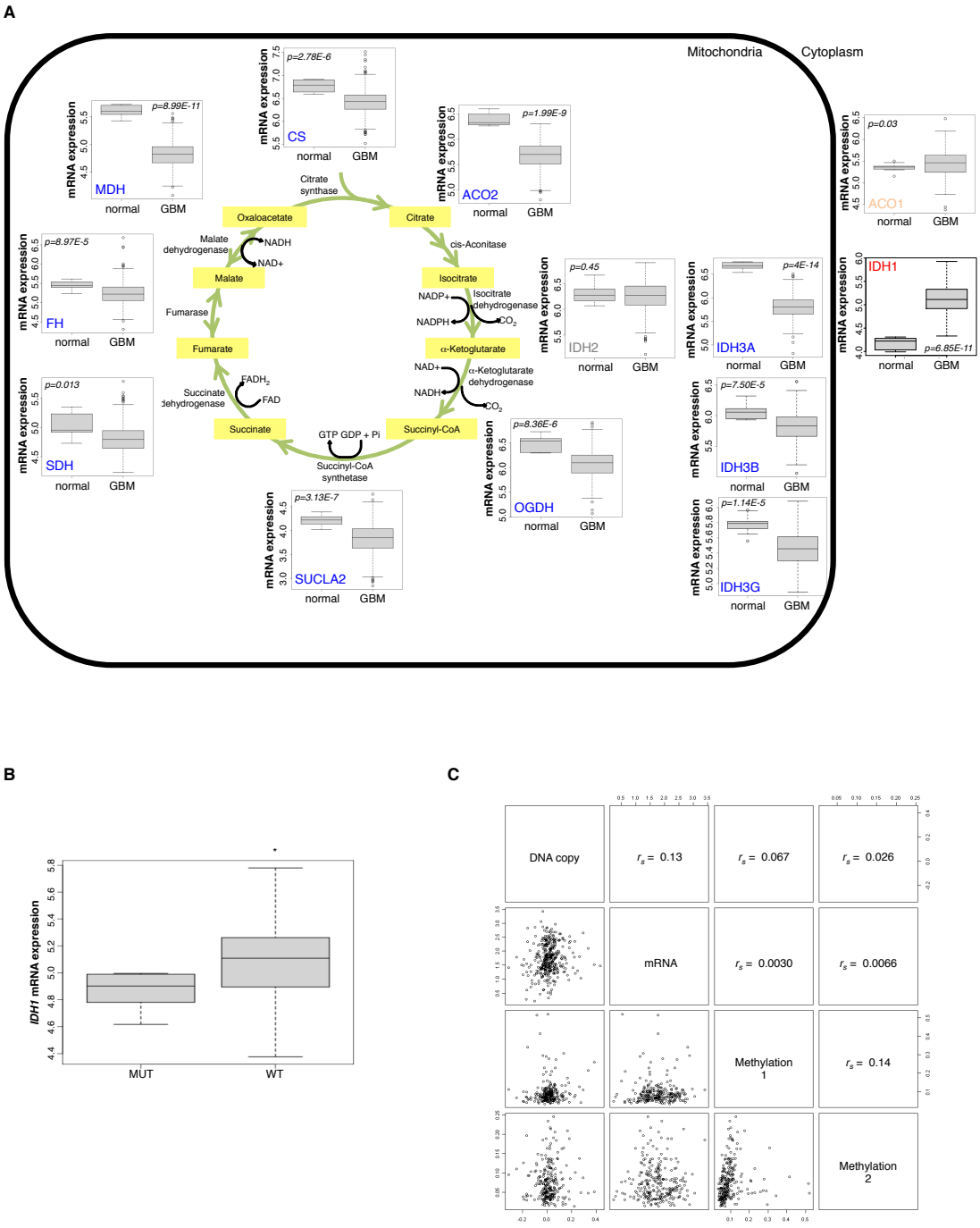

Figure S1. Related to Figure 1. TCA cycle enzyme mRNA expression in normal brain vs. GBM and elevated levels of IDH1 are not associated with copy number gains, amplification, or promoter methylation. (**A**) mRNA expression of *IDH1, IDH2, IDH3A, IDH3B, IDH3G, OGDH, SUCLA2, SDH, FH, MDH, CS, ACO1,* and *ACO2* in TCGA GBM *(n=420)* verses normal brain *(n=10)*. (**B**) mRNA expression of IDH1 in $IDH1^{R132H}$ mutant *(n=8)* vs. $IDH1^{wt}$ *(n=139)* GBM tumors. (**C**) TCGA dataset

analysis of *IDH1* mRNA, DNA copy number, and promoter methylation *(n=419)*. * *p= 0.00168;* ** *p= 0.06.* IDH1, isocitrate dehydrogenase 1; IDH2, isocitrate dehydrogenase 2; IDH3A, isocitrate dehydrogenase 3-alpha; IDH3B, isocitrate dehydrogenase 3-beta; IDH3G, isocitrate dehydrogenase 3-gamma; OGDH, α-ketoglutarate dehydrogenase; SUCLA2, succinyl-CoA synthetase; SDH, succinate dehydrogenase; FH, fumarase; MDH, malate dehydrogenase; CS, citrate synthase; ACO1, aconitase 1; ACO2, aconitase 2; r_s, spearman correlation coefficients.

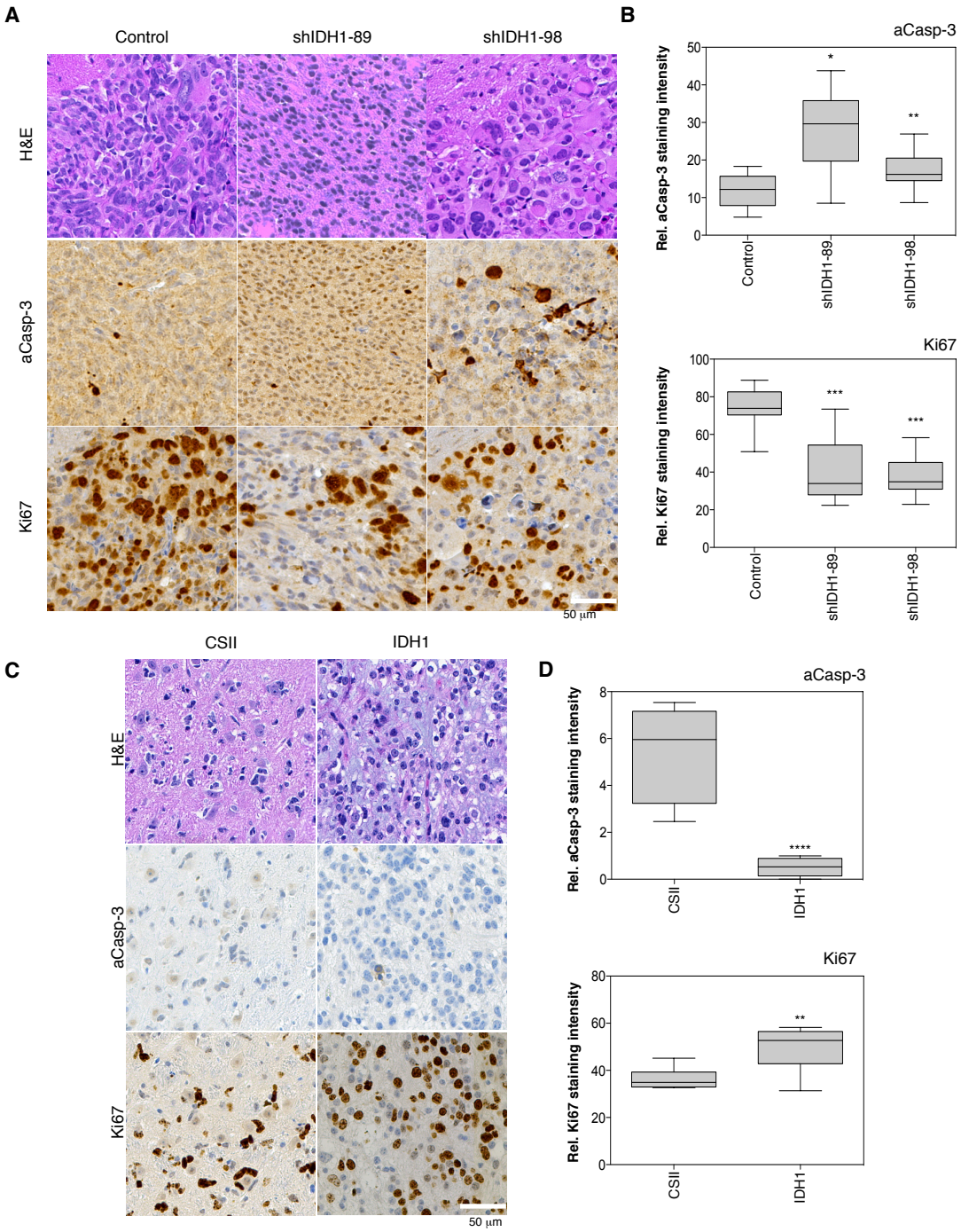

Figure S2. Related to Figure 2. Knockdown of IDH1 results in increased apoptosis and decreased cell proliferation while overexpression of IDH1 results in decreased apoptosis and increased cell proliferation *in vivo*. (**A**) Histopathological analysis of GIC-20 pLKO and shIDH1 tumors by H&E staining, IHC for aCasp-3 (apoptosis) and Ki67 (proliferation). Bar, 50 µm. (**B**) Quantification of aCasp-3 and Ki67 staining intensities by LSC *(5 independent areas in 3 independent tumors per group were counted; Mean ± SD)*. (**C**) Histopathological analysis of NSC tumors by H&E staining, IHC for aCasp-3 (apoptosis) and Ki67 (proliferation). Bar, 50 µm. (**D**) Quantification of aCasp-3 and Ki67 staining intensities by LSC *(6 independent areas in 1 tumor per group were counted; Mean ± SD)*. * *p<0.0005; ** p<0.05; *** p<0.0001; **** p<0.005.*

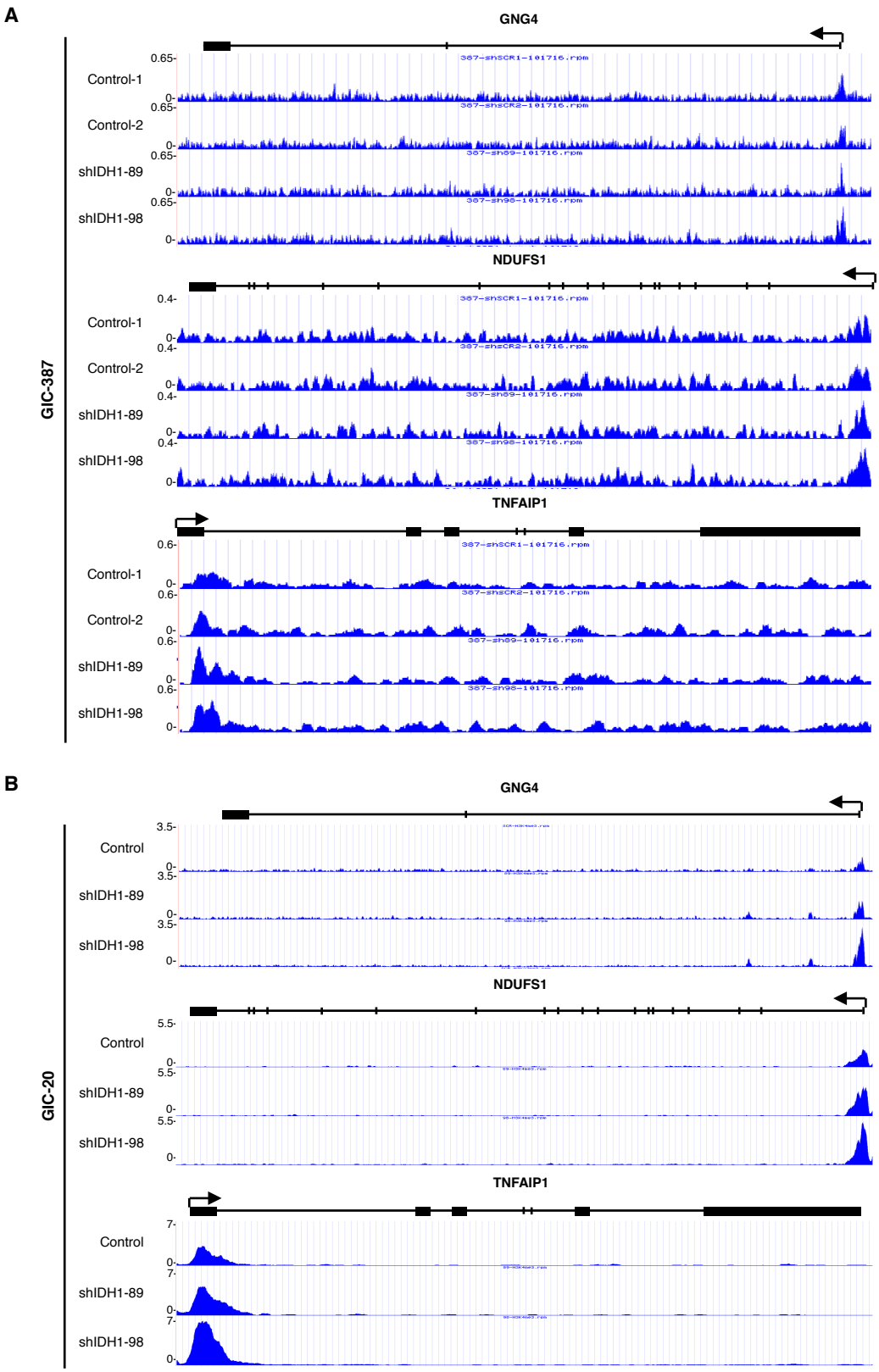

Figure S3. Related to Figure 4. Increased H3K4me3 binding at promoter regions of tumor suppressor genes. Genome tracks of tumor suppressor genes *GNG4*, *NDUFS1*, and *TNFAIP1* in GIC-387 (**A**) and GIC-20 (**B**) shScramble or shIDH1 infectants.

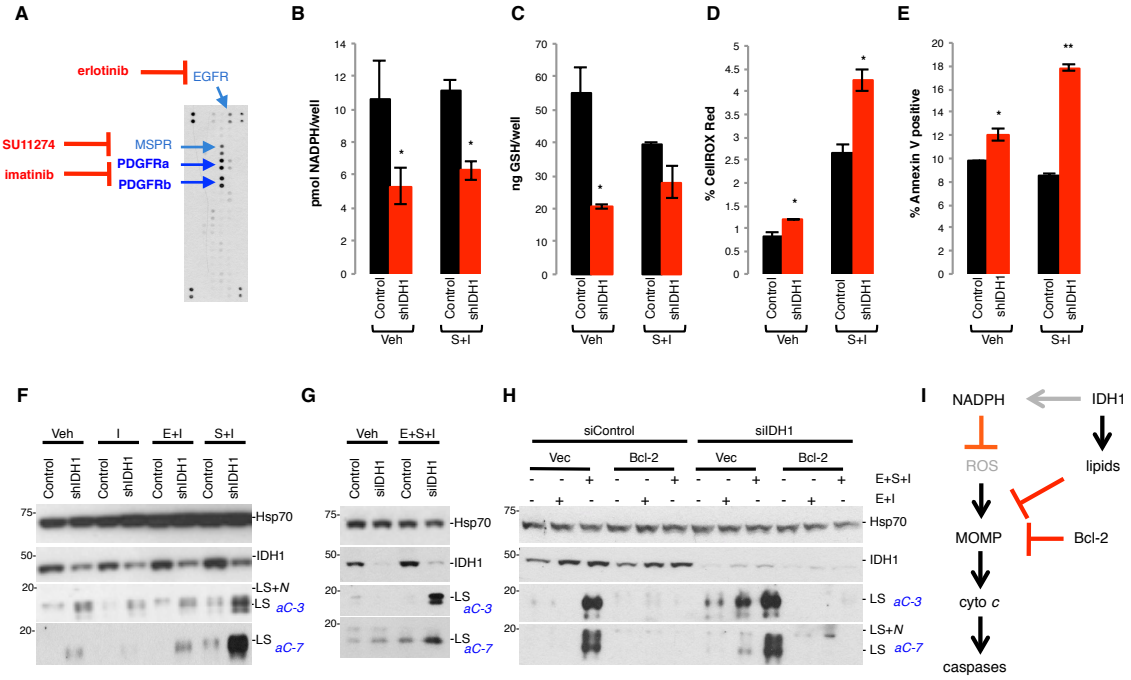

Figure S4. Related to Figure 5. Knockdown of IDH1 sensitizes transformed glioma cells harboring co-activation of multiple RTKs toward RTKi. (**A**) Phospho-tyrosine RTK antibody array in LN382 cells *(representative of 4 independent experiments)*. (**B**) NADPH *(representative of 4 cultures; Mean ± SD)*, (**C**) GSH *(representative of 5 cultures; Mean ± SD)*, and (**D**) ROS levels *(3 cultures per group; Mean ± SD)* were quantified in vehicle (Veh)- and RTKi-treated control (pLKO or shScramble), or shIDH1-infected LN382 cells. (**E**) FACS-based quantification of Annexin V positivity of RTKi-treated versus vehicle-treated LN382 cells expressing shScramble and shIDH1 cultures *(3 cultures per group; Mean ± SD)*. Effector caspase activation as determined by western blotting of LN382 expressing shScramble or shIDH1 (**F**) *(representative of 7 independent experiments)* or siScramble or siIDH1 (**G**) *(representative of 4 independent experiments)* treated with RTKi. (**H**) Western blot for active effector caspases in LN382 overexpressing Bcl-2, transiently transfected with siRNA targeted to IDH1, and treated with an RTKi cocktail *(representative of 2 independent experiments)*. (**I**) IDH1 pro-apoptotic effects are upstream of mitochondrial dysfunction. * $p<0.05$; ** $p<0.005$. MOMP, mitochondrial outer membrane permeabilization; cyto *c*, cytochrome *c*; E, erlotinib; S, SU11274; I, imatinib; LS, large subunit; LS+*N*, large subunit plus *N*-peptide.

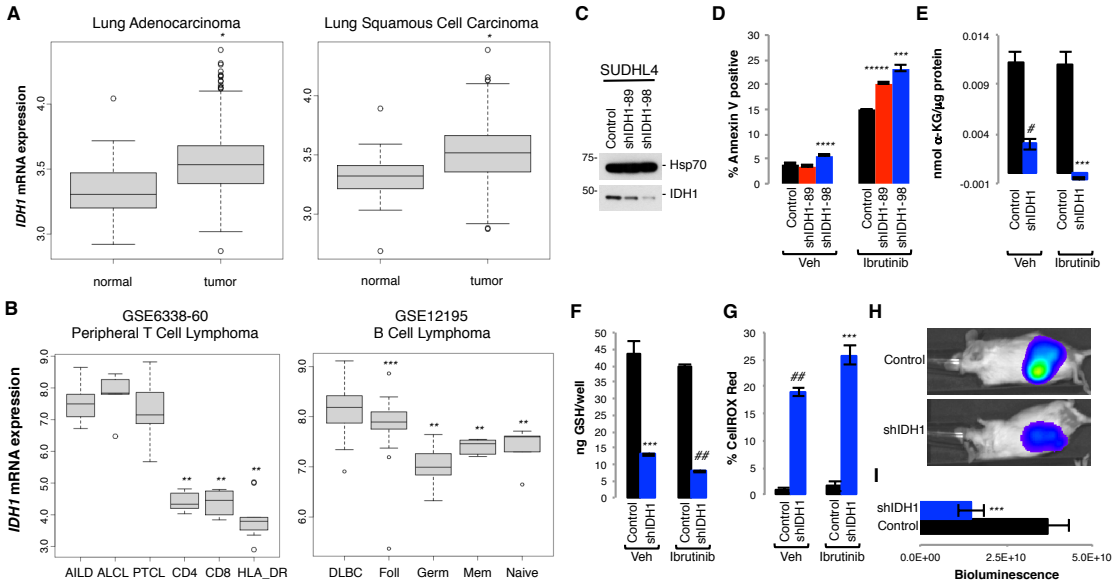

Figure S5. Related to Figure 5. IDH1 protects cancer cells derived from non-glioma tumors from apoptosis. (**A**) TCGA dataset analysis of *IDH1* mRNA in lung adenocarcinoma *(n=488)* and lung squamous cell carcinoma *(n=489)* compared to normal lung tissue *(n=50)*. (**B**) *IDH1* mRNA expression in AILD *(n=6)*, ALCL *(n=6)*, and PTCL *(n=28)* in comparison to CD4 *(n=5)*, CD8 *(n=5)* or HLA-DR-positive T cells *(n=10),* and in DLBCL *(n=73)* in comparison to Foll *(n=38)*, Germ *(n=10)*, Mem *(n=5)* or naive B cells *(n=5)*. (**C**) The diffuse large B cell lymphoma cell line SUDHL4 was lentivirally transduced with pLKO or shRNAs targeted to IDH1, and IDH1 protein levels were assessed by western blotting. (**D**) Annexin V positivity *(3 cultures per group; Mean ± SD)*, (**E**) α-KG *(1 culture per group; Mean ± SD)*, (**F**) GSH *(1 culture per group; Mean ± SD)*, and (**G**) ROS levels *(3 cultures per group; Mean ± SD)* were quantified in vehicle (Veh)- or ibrutinib-treated pLKO and shIDH1 cultures. (**H, I**) Bioluminescence of SUDHL4 pLKO and shIDH1 cells 14 days after flank implantation in SCID mice *(n=5 animals per group; Mean ± SEM)*. * $p<5x10^{-10}$, ** $p<1x10^{-5}$, *** $p<0.005$, **** $p<0.05$, ***** $p<0.001$, # $p<0.01$, ## $p<0.0005$. AILD, angioimmunoblastic lymphadenopathy; ALCL, anaplastic large cell lymphoma; PTCL, peripheral T-cell lymphoma; DLBCL, diffuse large B cell lymphoma; Foll, follicular; Germ, germinal; Mem, memory.

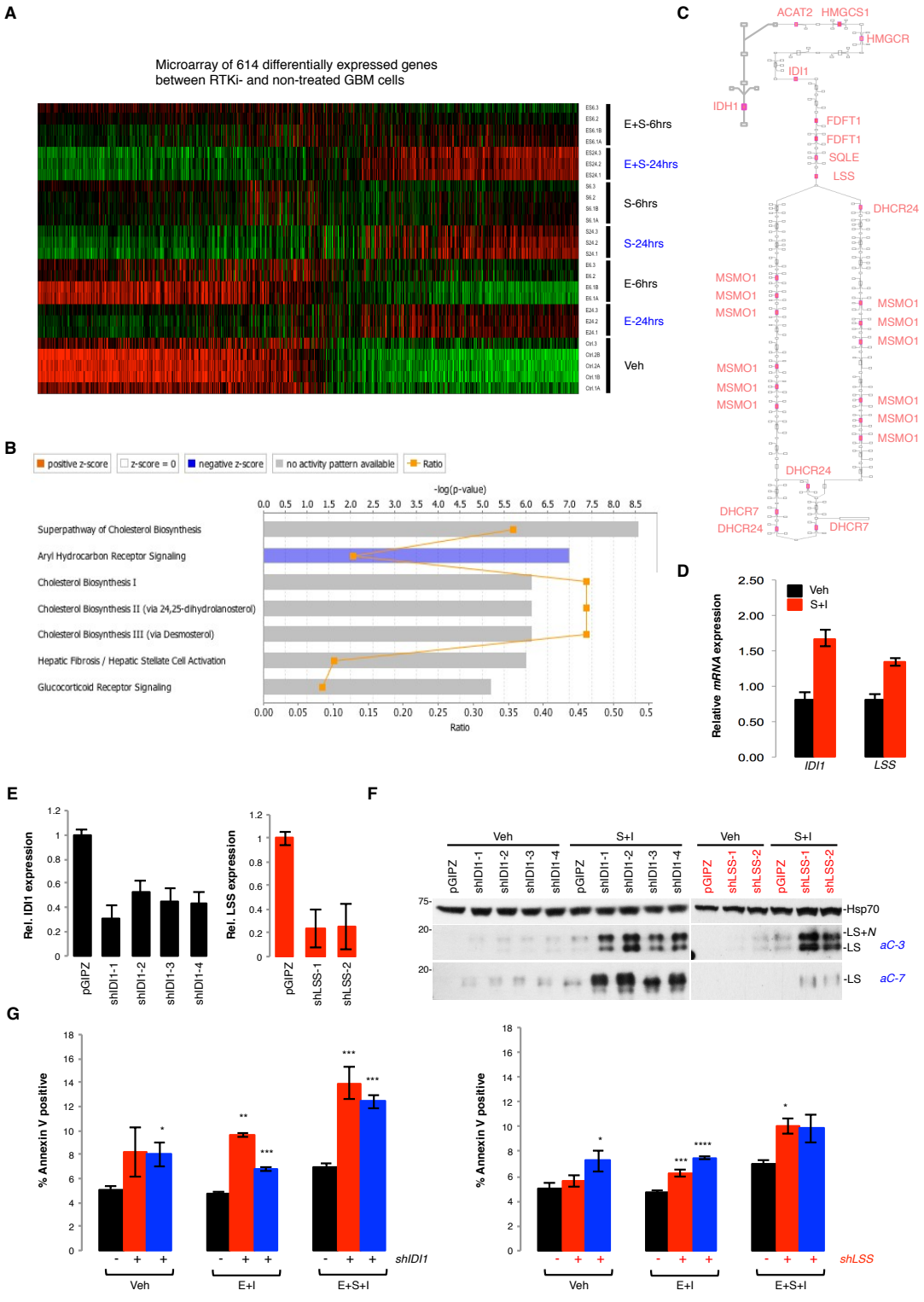

Figure S6. Related to Figure 6. Transcriptomic survey of RTKi-treated and untreated LN382 cells point to lipid biosynthesis as a major roadblock to RKi-treatment. (**A**) Microarray comparing LN382 cells treated with vehicle (Veh) or indicated RTKi cocktails. (*p<0.01*, *fold change (fc)>2*; *false discovery rate (fdr)>0.05*). (**B**) Ingenuity pathway analysis of differentially expressed (DE) genes points to cholesterol biosynthesis as a critical pathway differentially regulated by RTKi treatment. (**C**) Schematic of

the cholesterol synthesis pathway. Highlighted in red are enzymes upregulated on mRNA level upon RTKi treatment. (**D**) RT-qPCR-based quantification of *IDI1* and *LSS* mRNA expression in vehicle versus RTKi-treated cells *(representative of 3 independent experiments)*. (**E**) *IDI1* and *LSS* mRNA expression was assessed by RT-qPCR using total RNA isolated from LN382 cells infected with shRNAs targeting either *IDI1* or *LSS (representative of 2 independent experiments)*. (**F**) LN382 cells modified for reduced IDI1 or LSS expression were treated with vehicle (Veh) or RTKi, and effector caspase activation was assessed by western blot analysis *(representative of 2 independent experiments)*. (**G**) LN382 stably expressing shRNAs targeted to IDI1 and LSS were treated with the indicated combinations of RTKi, and Annexin V positivity was quantified by FACS *(3 cultures per group; Mean ± SD). * $p<0.05$; ** $p<0.001$; *** $p<0.01$; **** $p<0.005$*. E, erlotinib; S, SU11274; I, imatinib; ACAT2, acetyl-CoA acetyltransferase 2; HMGCS1, 3-hydroxy-3-methylglutaryl-CoA synthase 1; HMGCR, 3 hydroxy-3-methylglutaryl-CoA reductase; IDI1, isopentenyl-diphosphate delta isomerase 1; FDFT1, farnesyl-diphosphate farnesyltransferase 1; SQLE, squalene epoxidase; LSS, lanosterol synthase; DHCR24, 24-dehydrocholesterol reductase; MSMO1, methylsterol monooxygenase; DHCR7, 7-dehydrocholesterol reductase; LS, large subunit; LS+*N*, large subunit plus *N*-peptide.

Supplemental Tables:

Table S1. Related to Figure 4. List of top genes with differential H3K4me3 binding between control and shIDH1-expressing GIC-387.

Table S2. Related to Figure 6. List of differentially expressed genes by micro-array in RTKi- versus vehicle-treated LN382 cells.

Supplemental Experimental Procedures:

IDH1 genomic and genetic analysis

a. Preprocessing of TCGA GBM exon-array data and subtyping
The unprocessed Affymetrix exon-array datasets for 419 GBM samples and 10 normal brain samples (control samples) were downloaded from the TCGA data portal (https://tcga-data.nci.nih.gov/tcga). We followed the data preprocessing procedure described in our recent study (Pal et al., 2014). Samples underwent subtyping into one of 4 molecular classes of GBM (classical, mesenchymal, proneural, and neural) (Verhaak et al., 2010). We used an isoform-based classifier to obtain the patient subtype information (Pal et al., 2014).

b. Analysis of TCGA GBM, LGG, LUAD, and LUSC RNA-Seq data
RNASeqV2 level 3 released gene level expression data for RNA-seq were downloaded for GBM, LGG, LUAD and LUSC from TCGA, and for the analysis of IDH1 transcript levels in lymphoma from GSE12195 (Compagno et al., 2009) and GSE6338-60 (Piccaluga et al., 2007). The TCGA data processing and quality control were done by the Broad Institute's TCGA workgroup. The reference gene transcript set was based on the HG19 UCSC gene standard track. MapSplice (Wang et al., 2010) was used to do the alignment, and RSEM (Li and Dewey, 2011) to perform the quantitation. Student's t-test was used to determine whether TCA cycle genes were differentially expressed between tumor and corresponding normal. The upper quartile normalized RSEM count estimates were base-10 log transformed before the t-test.

c. TCGA GBM mutation data
We obtained level 2 GBM somatic mutation data from the TCGA web site (http://tcga-data.nci.nih.gov/tcga/). All non-silent *IDH1* and *EGFR* mutations were used. There were a total of 147 samples for which both expression and mutation data were available.

RT-qPCR

GBM tumor samples were acquired from patients having undergone surgery at Northwestern Memorial Hospital (NMH) in compliance with the NMH Institutional Review Board. To analyze *IDH1* expression levels in glioma tumor samples, RT-qPCR was performed using cDNA isolated from GBM tumor samples. Expression of *IDH1* in glioma tumors was compared with a normal brain reference pool consisting of 23 individual brain samples (FirstChoice Human Brain Reference, catalog no. AM6050; Life Technologies). cDNA of matched CD133+ and CD133- patient samples was obtained from Dr. Jeremy Rich (Cleveland Clinic). Total RNA from tumors or cell lines was extracted using RNeasy kit (Qiagen) according to manufacturer's protocol. cDNA was reversed transcribed (500 ng of total RNA as template) using M-MLV Reverse Transcriptase reactions (Promega), according to the manufacturer's protocol. qPCR was performed using either SYBR Green technology or TaqMan Probes (Life Technologies). The following primers were used to amplify *IDH1*, *GNG4*, *NDUFS1*, *TNFAIP1*, *ETV6*, *TUSC2*, *IDI1*, *LSS*, and *SREBP1*, respectively using SYBER Green: *IDH1* (forward primer: GGCGAGCAGCACAGAGAC and reverse primer: TCACCCCAGATACCATCAGA); *GNG4* (forward primer: GAGGGCATGTCTAATAACAGCAC and reverse primer: AGACCTTGACCCTGTCCATAC); *NDUFS1* (forward primer: TTAGCAAATCACCCATTGGACTG and reverse primer: CCCCTCTAAAAATCGGCTCCTA); *TNFAIP1* (forward primer: ACCTCCGAGATGACACCATCA and reverse primer: GGCACTCTGGCACATATTCAC); *ETV6* (forward primer: GCTCAGTGTAGCATTAAGCAGG and reverse primer: CGAGGAAGCGTAACTCGGC); *TUSC2* (forward primer: GGAGACAATCGTCACCAAGAAC and reverse primer: TCACACCTCATAGAGGATCACAG); *IDI1* (forward primer: GGCGAGCAGCACAGAGAC and reverse primer: TCACCCCAGATACCATCAGA); *LSS* (forward primer: CTGAACGGGATGACATTTTACG and reverse primer: GGAAAAGTGGGCCACCATAA); SREBP1 (forward primer: CCCTGTAACGACCACTGTGA and reverse primer: ACAGTGGCTCCGTCTGTCTT); HPRT was used as a house keeping gene control (forward primer: AAGGACCCCACGAAGTGTTG and reverse primer: GCTTTGTATTTTGCTTTTCCA). qPCR using Taqman Universal PCR Master Mix (Life Technologies) was used for GFAP and Nestin using the following Taqman probes: GAPDH (Hs02758991_g1), GFAP

(Hs00909233_m1) and Nestin (Hs04187831_g1). All reactions were performed on a 7900HT Fast Real-Time PCR System (Applied Biosystems). Results were analyzed and mRNA expression quantified using the ΔΔCt method.

Immunohistochemistry and Analysis

University of Kentucky (UK)-TMA containing three 2-μm diameter cores per tumor were obtained, with each core embedded in a separate TMA block. A total of 104 cases comprised the UK-TMA, including 9 non-neoplastic controls (cortical dysplasias) and 47 grade IV GBMs. TMA visually semiquantified via light microscopy were ranked on a relative scale from 0 to 3, with 0 = negative and 3 = strongest. Results from all 3 cores were averaged together to produce a final score for a tumor. Results were plotted, and differences were calculated via one-way ANOVA with post-hoc Tukey's test. Paraffin-embedded mouse brains isolated from PDX mouse models were deparaffinized, and incubated with 3% hydrogen peroxide (to block endogenous peroxidases), avidin (to block endogenous biotin), and 5% normal donkey serum (to reduce unspecific antibody binding). PDX tumor slides were incubated with primary antibodies [1:1000 Ki67 (Abcam ab16667); and 1:500 Caspase-3 (Cell Signaling 9661)]. After primary antibody incubation, slides were incubated with secondary biotinylated antibodies (Vectastain ABC kit-Vector Laboratories), and finally with Biotinyl Tyramide Working solution, Streptavidin-HRP, and DAB. TMA slides were processed as described above, but antigen retrieval was done at 80°C for 1 hour (10mM sodium citrate, 0.1% Tween 20, pH 6). Representative photographs were taken using the TissueGnostics LSC system and analyzed using HistoQuest software.

Cell Culture

Transformed glioma cell lines (LN382, U87, and LNZ308) were from Dr. Webster Cavenee (University of California, San Diego) and normal human astrocytes (NHA) were from Dr. Russ Pieper (University of California, San Francisco). GIC-20 was a gift from Dr. Kenneth Aldape (University of M.D. Anderson Cancer Center). GIC-387 was a gift from Dr. Jeremy Rich (Cleveland Clinic). NSC-2201 were isolated by Dr. Hongwu Zheng (Cold Spring Harbor Laboratory). SUDHL4 diffuse large B-cell lymphoma cell line was a gift from Dr. Shad Thaxton. Primary human astrocytes were from ScienCell (#1800). Transformed glioma cell lines and NHA were grown in DMEM 1X with 4.5 g/L glucose, L-glutamine and sodium pyruvate (Corning), and supplemented with 10% fetal bovine serum (Life Technologies) and 1% PenStrep (Life Technologies). GICs were grown as neurospheres in DMEM/F12 50:50 with L-glutamine (Corning), supplemented with 1% PenStrep, B27 (Invitrogen), N2 (Invitrogen), human-Epidermal Growth Factor (hEGF; Shenandoah Biotech), Fibroblast Growth Factor (FGF; Shenandoah Biotech), Leukemia Inhibitory Factor (LIF; Shenandoah Biotech), and GlutaMAX (Life Technologies). SUDHL4 cells were grown in RPMI 1640 supplemented with 10% FBS and 1% PenStrep. Primary human astrocytes were grown in astrocyte media (ScienCell) supplemented with 1% astrocyte growth supplement (ScienCell) and 2% FBS (ScienCell). Cells were routinely tested for mycoplasma contamination using PlasmoTest (InvivoGen) according to the manufacturer's protocol. Cells grown under hypoxic conditions were grown in a 1.5% O_2 incubator. Cells were treated with the following drugs: 5 μM Erlotinib (Sigma), 5 μM SU11274 (Sigma), 5 μM Imatinib (Selleck Chemicals), 5 or 10 mM dimethyl α-ketoglutarate (Sigma), 0.5 mM *N*-Acetyl-L-Cysteine, 25 μM EUK-134 (Sigma), 1 μM Sodium Palmitate (Sigma), 100 μM Mevalonic Acid Lithium Salt (Sigma), or 7.5 μM Ibrutinib (ChemieTek), 50, 100, or 500 ng/mL EGF (Shenandoah), or 5, 10, 20, 25, 50, or 100 μM GSK864 (Sigma).

Lentiviral Production and Cell Infection

GIC, NSC, transformed glioma cells, and lymphoma cells were lentivirally transduced with pLKO.1-puro-CMV-tGFP, pLKO.1-puro-CMV-tGFP-SHC016 (shScramble), pLKO.1-CMV-tGFP-shIDH1 (TRCN000027284, TRCN000027289, TRCN000027298; Sigma-Aldrich), pGIPZ-puro, pGIPZ-puro-shIDI1 (V2LHS_48970, V2LHS_67394, V2LHS_67395, V2LHS_67396), pGIPZ-puro-shLSS (V2LHS_134081, V2LHS_134083), CSII-CMV-MCS-IRES2-Venus, CSII-CMV-MCS-IRES2-Venus-IDH1, or pLV-Tomato-IRES-Luciferase (Northwestern University SDRC DNA/RNA Delivery Core). IDH1 was cloned into CSII-CMV-MCS-IRES2-Venus vector using unique NheI and AgeI restriction sites.

293T cells were plated in T-175 flasks (75% confluence). Cells were then transfected using lipofectamine 2000 (Life Technologies) with 20 μg of lentiviral construct, 15 μg of psPAX2 (HIV-Gag-Pol-Rev), and 10 μg of pMD2.G (envelope). After 48-72 hrs, virus-containing media was harvested, filtered through 45 μm low protein binding filter (Millipore), and concentrated at 25,000 rpm for 2 hrs (Beckman Coulter). The resulting viral pellet was resuspended in 30 μL of serum free media. For lentiviral transduction, transformed cells at 75% confluence or GICs, NSCs, and lymphoma cells at $1x10^6$ cells per T-25 flask were incubated with 5 μL of virus for 48 hrs. Subsequently, cells were sorted by FACS to enrich for GFP-positive cells (pLKO, shIDH1, CSII, CSII-IDH1 constructs) or RFP-positive cells (luc), or puromycin-selected (pGIPZ, shIDI1, shLSS constructs).

Retroviral Production and Infection

Transformed glioma cells overexpressing Bcl-2 were generated by retroviral transduction using pBabe-puro or pBabe-puro-Bcl-2. pBABE-puro was obtained through Addgene (Addgene plasmid #1764; Morgenstern and Land, 1990). Bcl-2 was cloned into the pBabe-Puro retroviral vector using unique EcoRI restriction site. In a 10 cm dish, 40% confluent 293T cells in OptiMEM were transfected with 4 μg of retroviral construct, 1 μg of pVSVG (envelope), and 4 μg pCL-Ampho (packaging) using lipofectamine 2000 (Life Technologies). The medium was changed to full-DMEM medium 24 hrs post-transfection, and cells were incubated at 37°C for an additional 24 hrs. Medium was harvested, supplemented with Polybrene (8 μg/mL; Sigma-Aldrich), and filtered through a 0.45 μm filter. For retroviral infection, glioma cells at 50% confluence were incubated overnight with 3 mL of virus-containing medium. Cells were selected by changing the medium to puromycin-containing medium (1.5 μg/mL; Invitrogen).

Transfection

Subconfluent glioma cells were transfected with a non-targeting siRNA control or with an siRNA pool targeted to IDH1 (50 nM) or FoxO6 (100nM) (Dharmacon) using Oligofectamine or Lipofectamine 2000 (Invitrogen) according to the manufacturer's protocol. Subconfluent GIC-387 cells were transfected with a pCMV6-XL4-ME1 plasmid (Origene; 2 μg per well in 6 well plate) or mock transfected using RNAiMax (Invitrogen) according to the manufacturere's protocol. Expression analysis for FoxO6, IDH1, ME1, and cleaved effector caspases was performed 48 hrs post transfection.

***In vivo* Xenograft Studies**

All animals were used under an approved protocol of the Institutional Animal Care and Use Committee of Northwestern University. Luciferase-expressing GIC-20, GIC-387, and NSC-2201 cells were injected intracranially into ~7 week old female CB17 SCID mice (Taconic Farms). Briefly, cells were dissociated by accutase (Life Technologies), and suspended in HBSS. Each mouse was anesthetized and placed in a stereotaxic frame, and the surgical area was cleaned with alcohol and Betadine. An incision was made in the scalp, and a 0.7 mm burr hole was created in the skull with a microsurgical drill 2 mm lateral right of the sagittal suture and 0.5 mm posterior of bregma. A Hamilton syringe was loaded with $3x10^5$ cells (GIC-20), $2x10^3$ (GIC-287), or $4x10^5$ (NSC-2201) in 3 μL and inserted 3.5 mm into the brain. The cells were implanted over a period of 3 mins, and the needle was left in place for 1 min before the syringe was withdrawn. After surgery, the skin was closed with sutures. Mice were sacrificed upon observation of neurological impairment. 7-10 animals were used in each group. Mice were randomized to groups based on body weight. No blinding was possible in these studies. Survival analysis between control and experimental groups was determined by the Kaplan-Meier method, and statistical significance was assessed using the logrank (Mantel-Cox) test. For GSK864 inhibitor treatment, 20 animals were intracranially injected as described above with GIC-20.luc cells. Two weeks after implantation, mice were randomized into two groups based on bioluminescence from the IVIS spectrum. 10 animals received 150 mg/kg GSK864 (Sigma) in propylene glycol, DMSO, PEG-400, and water (16.7:3.3:40:40) or vehicle for 10 days, M-F for 2 weeks. For lymphoma flank model, $2x10^6$ cells in 100 μL of HBSS were combined with 100 μL of ice-cold Matrigel (Fischer Scientific). Mice were anesthetized and 200 μL of cells in Matrigel were injected into either the left flank (pLKO) or right flank (shIDH1-98) of 5 mice.

Carbon Labeling and Metabolite Studies

a. ^{13}Carbon Sample Preparation

GIC-20 cells were grown in medium supplemented with 10 mM glucose or 1 mM acetate until 90% confluence was reached. After 24 hrs, media was added, which contained either 10 mM [U-^{13}C] Glucose or 1 mM [U-^{13}C] Acetate (Cambridge Isotope Laboratories). After 3 hrs (acetyl-CoA) or 72 hrs (fatty acids), cells were collected and pelleted, washed without disturbing the pellet using 150 mM Ammonium Acetate, and snap frozen in liquid nitrogen. Samples were sent to University of Michigan Metabolomics Core for GC-MS processing. Microtubes containing cell pellets were removed from -80°C storage and maintained on wet ice throughout the processing steps. To initiate protein precipitation, 0.3 mL of a chilled mixture of isopropanol:chloroform (8:2) (EMD) was added to each sample. Extracted metabolites were dried under vacuum at 45°C, and 1 mL of BF3/Methanol was added to each sample. Samples were incubated at 60°C for 3 hrs and cooled. Subsequently, 200 μL LCMS water, and 300 μL of Hexane was added. The samples were vortexed, allowed to sit for 5 mins, vortexed again and then centrifuged for 3 mins to separate the layers. The organic layer was transferred to an autosampler vial for GC-MS analysis.

b. GC-MS

GC-MS analysis was performed on an Agilent 69890N GC-5975 MS detector with the following parameters: a 1 μL sample was injected splitlessly on an HP-5MS 15m column (Agilent Technologies) with an He gas flow rate of 1.4 mL/min. The GC oven initial temperature was 60°C, and was increased at 10°C per min to 300°C, and held at 300°C for 5 mins. The inlet temperature was 250°C and the MS-source and quad temperatures were 230° and 150°C respectively.

c. GC-MS Data Analysis

Metabolites were identified by matching the retention time and mass (+/- 10 ppm) to authentic standards. Isotope peak areas were integrated using MassHunter Quantitative Analysis vB.07.00 (Agilent Technologies). Peak areas were corrected for natural isotope abundance using an in-house written software package based on a method previously described (Fernandez et al., 1996), and the residual isotope signal was reported. Data were normalized to cell protein content prior to analysis of metabolite fluxes for fatty acid metabolites.

Chromatin Immunoprecipitation-Sequencing

GIC-387 cells were grown in 4 T75 flasks and infected with either shScramble, shIDH1-89, or shIDH-98 lentivirus. After 48 hrs, media was changed on the cells and they continued to grow. After 48 hrs more, 6 million cells per sample were fixed with 1% formaldehyde and ChIP-seq was performed according to previous studies (Chen et al., 2015-1 and Chen et al. 2015-2) using antibodies against H3K4me3 (Hu et al., 2013), H3K27me3 (Active Motif 39155), and H3K36me3 (Abcam ab9050). ChIP-Seq libraries were prepared with Illumina's TruSeq DNA sample preparation kit. Sequencing reads were aligned to the human genome (University of California at Santa Cruz [UCSC] hg19). Datasets were analyzed using Spatial Clustering for Identification of ChIP-Enriched Regions [SICER; (Xu et al., 2014)], to delineate ChIP-enriched regions, to assess their statistical significance, and to identify regions of differential enrichment in shIDH1 versus control GICs. For each antibody, regions detected by the SICER peak caller as reproducibly bound by the antibodies in at least one ChIP dataset were identified. The number of reads for each sample in each of these regions were then counted, and the R package edgeR (Robinson et al., 2010) was used to identify regions that significantly differed in H3K4me3, K27me3 and K36me3 binding between both shIDH1 infectants versus the control cultures. A p value of <0.05 was considered significant. Subsequently, Ingenuity Pathway Analysis (IPA; Qiagen) was performed to prioritize genes based upon enrichment in signaling pathways associated with cancer and development. Genes in the top 5 canonical pathways, as well as genes associated with pathways implicated in cellular and organismal development, were ranked based upon most significant differential in H3K4me3 binding between two independent shIDH1 infectants versus shCo cells (64 genes). Genes with annotated oncogenic or tumor-suppressive function (30 genes) were then analyzed by RT-qPCR.

Chromatin Immunoprecipitation

Chromatin Immunoprecipitations (ChIP) were performed using EZ-ChIP System (Millipore) according to manufacturer's protocol with slight modifications. LN382 cells were grown to 75% confluence in four 15 cm plates, treated with 5 μM SU11274 plus 5 μM Imatinib, or vehicle. After 48 hrs, DNA was sheared, and incubated with 5 μg of anti-FoxO6 (Thermo Scientific PA5-35117) or IgG Rabbit (Santa Cruz) overnight at 4°C. After washing, the DNA was eluted from the agarose beads twice and DNA was purified using the spin columns. qPCR was performed using the following primers for IDH1 (forward primer: TATACTCCAGCCTGGGCAAC and reverse primer: ACAGCCCCTAGGGTTCTTTG) and confirmed with an independent second set of IDH1 primers (forward primer: CTGAGATCACGCCACTATACTCCAGC and reverse primer: GCCCTTACCCCATGCATGAAACTTCC).

Microarray Analysis

LN382 cells were treated with erlotinib, SU11274, or a combination of both drugs for 6 or 24 hrs. Total RNA was extracted using RNeasy Kit (Qiagen). The quality of the RNA was evaluated by Bioanalyzer, and subjected to whole genome profiling using the Illumina HumanHT-12 Beadchip expression technology (Illumina). Cutoff conditions for significant gene changes were *fold change (fc)>2* , $p<0.01$, and *false discovery rate (FDR)>0.05.* Results were analyzed using Ingenuity Pathway Analysis (Qiagen).

***EGFR* Copy Number Alterations**

For the analysis of *EGFR* copy number in GICs, genomic DNA was isolated [Blood and Cell Culture DNA Mini Kit (Qiagen)], and 10 ng were analyzed using the TaqMan Copy Number Assay (Applied Biosystems) following the manufacturer's protocol. RNase P TaqMan was used as a reference.

RTK Array

RTK activation was determined using Human Phospho-RTK Array Kit (R&D Systems) according the manufacturer's protocol.

Supplemental References:

Chen, F.X., Woodfin, A.R., Gardini, A., Rickels, R.A., Marshall, S.A., Smith, E.R., Shiekhattar, R., Shilatifard, A. (2015a). PAF1, a molecular regulator of promoter-proximal pausing by RNA Polymerase II. Cell *162*, 1003-1015.

Chen, F., Gao, X., Shilatifard, A. (2015b). Stably paused genes revealed through inhibition of transcription initiation by the TFIIH inhibitor triptolide. Genes Dev. *29*, 39-47.

Compagno, M., Lim, W.K., Grunn, A., Nandula, S.V., Brahmachary, M., Shen, Q., Bertoni, F., Ponzoni, M., Scandurra, M., Califano, A., et al. (2009). Mutations of multiple genes cause deregulation of NF-kappaB in diffuse large B-cell lymphoma. Nature *459*, 717-721.

Fernandez, C.A., Des Rosiers, C., Previs, S.F., David, F., and Brunengraber, H. (1996). Correction of 13C mass isotopomer distributions for natural stable isotope abundance. J. Mass Spectrom. *31*, 255-262.

Hu, D., Garruss, A.S., Gao, X., Morgan, M.A., Cook, M., Smith, E.R., Shilatifard, A. (2013). The MII2 branch of the COMPASS family regulates bivalent promoters in mouse embryonic stem cells. Nat. Struct. Mol. Biol. *20*, 1093-1097.

Li, B., and Dewey, C.N. (2011). RSEM: accurate transcript quantification from RNA-Seq data with or without a reference genome. BMC Bioinformatics *12*, 323.

Morgenstern, J.P. and Land, H. (1990). Advanced mammalian gene transfer: high titre retroviral vectors with multiple drug selection markers and a complementary helper-free packaging cell line. Nucleic Acids Res. *18*, 3587-3596.

Pal, S., Bi, Y., Macyszyn, L., Showe, L.C., O'Rourke, D.M., and Davuluri, R.V. (2014). Isoform-level gene signature improves prognostic stratification and accurately classifies glioblastoma subtypes. Nucleic Acids Res. *42*, e64.

Piccaluga, P.P., Agostinelli, C., Califano, A., Rossi, M., Basso, K., Zupo, S., Went, P., Klein, U., Zinzani, P.L., Baccarani, M., et al. (2007). Gene expression analysis of peripheral T cell lymphoma, unspecified, reveals distinct profiles and new therapeutic targets. J. Clin. Invest. *117*, 823-834.

Robinson, M.D., McCarthy, D.J., and Smyth, G.K. (2010). edgeR: a bioconductor package for differential expression analysis of digital gene expression data. Bioinformatics *26*, 139-140.

Unruh, D., Schwarze, S.R., Khoury, L., Thomas, C., Wu, M., Chen, L., Liu, Y., Schwartz, M.A., Amidei, C., Kumthekar, P., et al. (2016). Mutant IDH1 and thrombosis in gliomas. Acta. Neuropathol. *132*, 917-930.

Verhaak, R.G., Hoadley, K.A., Purdom, E., Wang, V., Qi, Y., Wilkerson, M.D., Miller, C.R., Ding, L., Golub, T., Mesirov, J.P. et al. (2010). Integrated genomic analysis identifies clinically relevant subtypes of glioblastoma characterized by abnormalities in PDGFRA, IDH1, EGFR, and NF1. Cancer Cell *17*, 98-110.

Wang, K., Singh, D., Zeng, Z., Coleman, S.J., Huang, Y., Savich, G.L., He, X., Mieczkowski, P., Grimm, S.A., Perou, C.M., et al. (2010). MapSplice: accurate mapping of RNA-seq reads for splice junction discovery. Nucleic Acids Res. *38*, e178.

Xu, S., Grullon, S., Ge, K., and Peng, W. (2014). Spatial clustering for identification of ChIP-enriched regions (SICER) to map regions of histone methylation patterns in embryonic stem cells. Methods Mol. Biol. *1150*, 97-111.